Supporting information

Size-Dependent Magnetomechanically Enhanced Photothermal Antibacterial Effect of Fe_3O_4@Au/PDA NanoDurian

*Yunqi Xu[a, 1], Kang Wang[a, 1], Yi Zhu[b, *], Jing Wang[c], Dazheng Ci[c], Min Sang[a], Qunling Fang[c], Huaxia Deng[a], Xinglong Gong[a, *], Ken Cham-Fai Leung[d], Shouhu Xuan[a, *]*

[a] CAS Key Laboratory of Mechanical Behavior and Design of Materials, Department of Modern Mechanics, University of Science and Technology of China, Hefei 230027, PR China

[b] Department of Obstetrics and Gynecology, The First Affiliated Hospital of University of Science and Technology of China, Hefei, China.

[c] School of Food and Biological Engineering, Hefei University of Technology, Hefei, 230009, PR China

[d] State Key Laboratory of Environmental and Biological Analysis, Department of Chemistry, The Hong Kong Baptist University, Kowloon, Hong Kong SAR, PR China

[1]*These authors contributed to this work equally and should be regarded as co-first authors.*

*Corresponding author:
Prof. Xinglong Gong
E-mail: gongxl@ustc.edu.cn
Tel: 86-551-63600419
Fax: 86-551-63600419

Dr. Yi Zhu
E-mail: yizhu@ustc.edu.cn

Prof. Shouhu Xuan
E-mail: xuansh@ustc.edu.cn
Tel: 86-551-63601702
Fax: 86-551-63606382

This file includes:

Simulation model: Modified formulae for the magnetic dipolar force, van der Waals force, and hydrodynamic drag force were employed in the simulation model.

Table S1. The weight percentage of the Au and Fe elements in the different samples

Figures S1 to S9

Video S1: Differences in magnetic separation of small and large particles

Video S2: With or without sample constantly move under the influence of a magnetic field.

Video S3: Observation of the structure of S-Fe_3O_4@Au/PDA under a rotating magnetic field.

Video S4: Observation of the structure of L-Fe_3O_4@Au/PDA under a rotating magnetic field

Video S5: Microscopic Observation of S-Fe_3O_4@Au/PDA on Biofilm Treatment of *Staphylococcus aureus* Under a Rotating Magnetic Field

Video S6: Microscopic Observation of L-Fe_3O_4@Au/PDA on Biofilm Treatment of *Staphylococcus aureus* Under a Rotating Magnetic Field

Simulation model

Simulation set-up

Periodic boundary conditions were applied in the x-z and y-z planes, while shear boundary conditions were applied in the x-y plane. The number of particles was kept constant at N=2,000. Initially, the particles were randomly distributed in the simulation box with a fixed direction along the Z-axis. An external magnetic field along the Z-axis and a steady shear flow along the X-axis were suddenly applied. The simulation started and continued until the shear stress reached an equilibrium state. To reduce computational time, the simulation terminated at t=40 ms.

Inter-particle forces

The relationship between magnetization M and external field strength H of super-paramagnetic Fe_3O_4 and Fe_3O_4@Au/PDA can be characterized by the Langevin function:

$$M = M_s\left[\coth\left(\frac{H}{x}\right) - \frac{x}{H}\right] \tag{1}$$

where $x = M_sV_p/k_BT$. M_s means the saturation magnetization. Thus, the magnetic moment induced by the external field can be determined as:

$$\boldsymbol{m}_i = MV_p\frac{\boldsymbol{H}}{H} \tag{2}$$

where V_p represents the volume of the particles. $H = |\boldsymbol{H}|$.

After magnetized by the external field, particle i will generate a magnetic field at the position of particle j:

$$\boldsymbol{H}_i = -\frac{1}{4\pi r_{ij}^{\,3}}\left[\boldsymbol{m}_i - 3(\boldsymbol{m}_i\cdot\hat{\boldsymbol{r}})\hat{\boldsymbol{r}}\right] \tag{3}$$

where r_{ij} denotes a spatial vector from the center of particle i to the spatial point. $r = |r|$ and $\hat{r} = \boldsymbol{r}/r$.

According to the point-dipole model, the magnetic force imposed on particle i exerted by particle j is given by:

$$\boldsymbol{F}_{ij}^{\mathrm{m}}=\frac{3\mu_0}{4\pi r_{ij}^{\ 4}}c_{\mathrm{m}}\left[\left(-\boldsymbol{m}_i\cdot\boldsymbol{m}_j+5\boldsymbol{m}_i\cdot\hat{\boldsymbol{r}}\ \boldsymbol{m}_j\cdot\hat{\boldsymbol{r}}\right)\hat{\boldsymbol{r}}-\left(\boldsymbol{m}_i\cdot\hat{\boldsymbol{r}}\right)\boldsymbol{m}_j-\left(\boldsymbol{m}_j\cdot\hat{\boldsymbol{r}}\right)\boldsymbol{m}_i\right] \tag{4}$$

Here, the magnetic permeability of the matrix is approximately equal to $\mu_0=4\pi\times10^{-7}$ N/A^2. c_{m} is a factor to correct the dipole model when two particles are very close to each other.

The van der Waals force between two particles is expressed as:

$$\boldsymbol{F}_{ij}^{\mathrm{vdW}}=\frac{A}{6}L_{ij}d^2\left[\frac{1}{L_{ij}^{\ 2}-d^2}-\frac{1}{L_{ij}^{\ 2}}\right]^2\hat{\boldsymbol{r}} \tag{5}$$

The Hamaker constant is A=3×10^{-20} J. L_{ij}=max [r_{ij}, 1.01d]. d is the average diameter of magnetic particles. In order to avoid the overlap of particles, an exponential repulsive force is introduced as:

$$\boldsymbol{F}_{ij}^{\mathrm{r}}=-\left(\frac{3\mu_0 M_{\mathrm{s}}^{\ 2}V_{\mathrm{p}}^{\ 2}}{2\pi d^4}+\boldsymbol{F}_{ij}^{\mathrm{vdw}}\right)10^{-10\left(\frac{r_{ij}}{d}-1\right)}\hat{\boldsymbol{r}} \tag{6}$$

The random Brownian force acting on each particle is described as:

$$\boldsymbol{F}_i^{\mathrm{B}}=\boldsymbol{R}\sqrt{\frac{6\pi k_{\mathrm{B}}Td\eta}{\delta t}} \tag{7}$$

where $\boldsymbol{R}$ is a unit random vector whose components are Gaussian numbers with zero mean. k_{B} is the Boltzmann constant. The time interval of the Brownian force is chosen as $\delta_t = 0.1\tau_{\mathrm{p}}$. $\tau_{\mathrm{p}} = d^2\rho_{\mathrm{p}}/18\eta$ is the characteristic time of particles and ρ_{p} is the density of particles. η is the viscosity of the matrix. It is noted that the integral of this random force over a long time is independent on the choice of δt.

Governing equations

In a magnetic fluid, the motion of magnetic particles relative to the matrix belongs to Stokes flow with a Reynolds number of Re=0. Therefore, the hydrodynamic drag force can be modelled by Stokes law:

$$\boldsymbol{F}_i^{\mathrm{h}}=-3\pi\eta dc_{\mathrm{h}}\left(\boldsymbol{v}_i-\boldsymbol{u}_i\right) \tag{8}$$

where *vi-ui* is the velocity of particle i relative to the matrix. In concentrated magnetic fluid, the surrounding particles will enlarge the drag force. c_h is a correction factor for $\boldsymbol{F}_i^{\mathrm{h}}$, presented as:

$$c_{\mathrm{h}} = \frac{1+5.81\varphi}{(1-\varphi)^3} + 0.48\frac{\sqrt[3]{\varphi}}{(1-\varphi)^4} + \varphi^3 \,\mathrm{Re}\left[0.95 + \frac{0.61\varphi^3}{(1-\varphi)^2}\right] \tag{9}$$

Here, φ is the volume fraction of magnetic fluid. The magnetic torque acting on a single particle is so exiguous that the rotational motion is neglectable. Considering the forces mentioned above, the equation of motion is constructed as:

$$\sum_{j\neq i}\left(\boldsymbol{F}_{ij}^{\mathrm{m}} + \boldsymbol{F}_{ij}^{\mathrm{vdW}} + \boldsymbol{F}_{ij}^{\mathrm{r}}\right) + \boldsymbol{F}_i^{\mathrm{B}} + \boldsymbol{F}_i^{\mathrm{h}} = m_{\mathrm{p}i}\boldsymbol{a}_i \tag{10}$$

Where $m_{\mathrm{p}i}$ is the mass of particle *i*.

The modified velocity-Verlet algorithm is employed to solve Eq. 10, in which the empirical parameter is chosen as 0.65. The magneto-induced stress tensor $\boldsymbol{\sigma}$ and magnetic potential energy U_{m} are presented as:

$$\boldsymbol{\sigma} = \frac{1}{V}\sum_i\left[\sum_{j>i}\boldsymbol{r}_{ij}\boldsymbol{F}_{ij} - m_{\mathrm{p}i}\left(\boldsymbol{v}_i - \boldsymbol{u}_i\right)\left(\boldsymbol{v}_i - \boldsymbol{u}_i\right)\right] \tag{11}$$

$$U_{\mathrm{m}} = \mu_0\sum_i\left[-\boldsymbol{m}_i\cdot\boldsymbol{H} + \sum_{j>i}\frac{1}{4\pi r_{ij}^{\,3}}\left(\boldsymbol{m}_i\cdot\boldsymbol{m}_j - 3\boldsymbol{m}_i\cdot\hat{\boldsymbol{r}}\;\boldsymbol{m}_j\cdot\hat{\boldsymbol{r}}\right)\right] \tag{12}$$

Here, V is the volume of the simulation box. $\boldsymbol{F}_{ij}$ is the total inter-particle force between these two particles. U_{m} consists of the particle-external field section and inter-particle section.

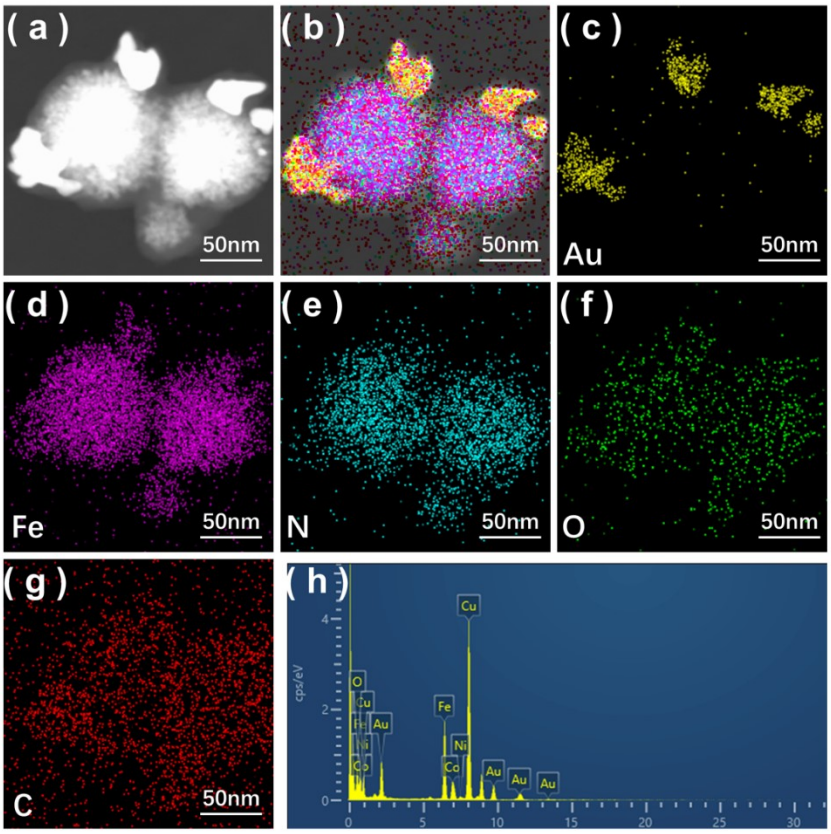

Figure S1. HAADF-STEM images (a) and EDX elemental mapping of Au, Fe, N, O and C (b–g) and the EDX spectrum (h) of the S-Fe_3O_4@Au/PDA. Scale bar is 50 nm.

Table S1. The weight percentage of the Au and Fe elements in the different samples

	Au (wt%)	**Fe (wt%)**
L-Fe_3O_4		**53.35**
L-Fe_3O_4@Au/PDA	**18.14**	**33.83**
S-Fe_3O_4		**59.25**
S-Fe_3O_4@Au/PDA	**19.49**	**37.07**

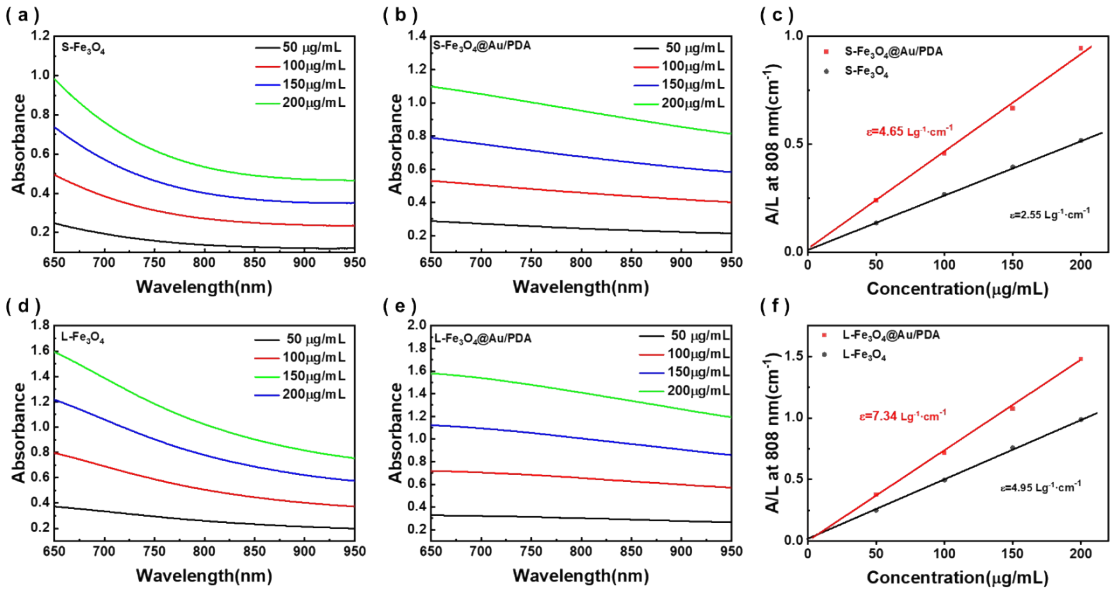

Figure S2. UV–vis spectra of different concentrations of S-Fe_3O_4 (a), S-Fe_3O_4@Au/PDA (b), L-Fe_3O_4 (d) and L-Fe_3O_4@Au/PDA (e) dispersed in aqueous solution; (c) and (f) the extinction coefficient of different samples.

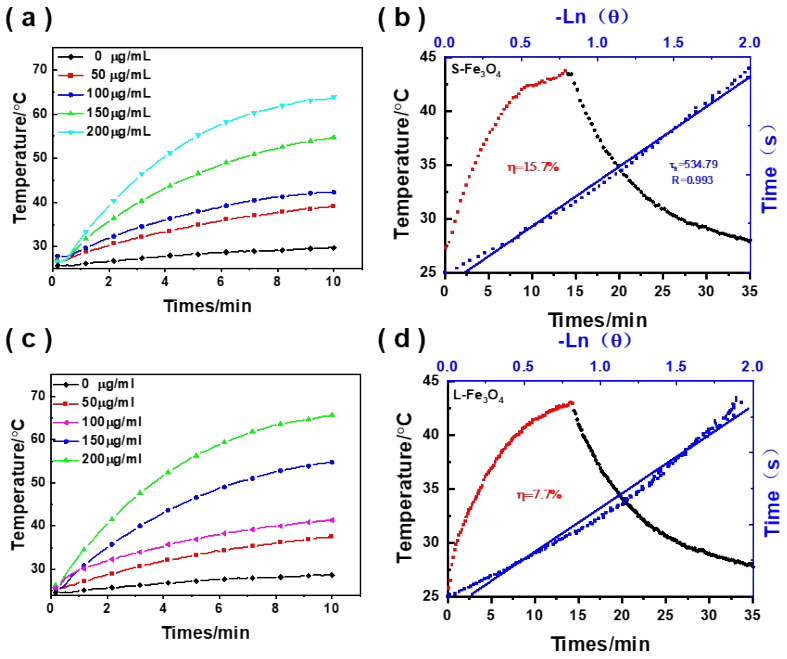

Figure S3. Temperature elevation of S-Fe_3O_4 (a) and L-Fe_3O_4 (b) with different concentrations. Temperature elevation curves of S-Fe_3O_4 (c) and L-Fe_3O_4 (d) suspension after continuous irradiation and natural cooling and a plot fitting of cooling time *vs* -ln(θ) (100 μg/mL).

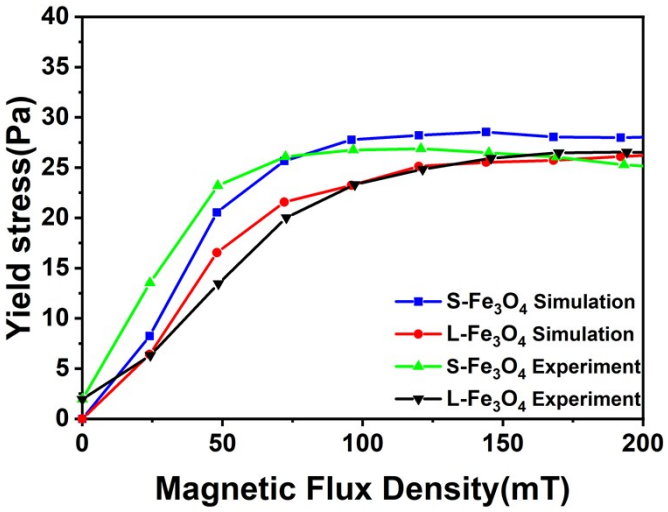

Figure S4. Comparison of experimental and simulated results of magnetic field sweep test (25 wt%).

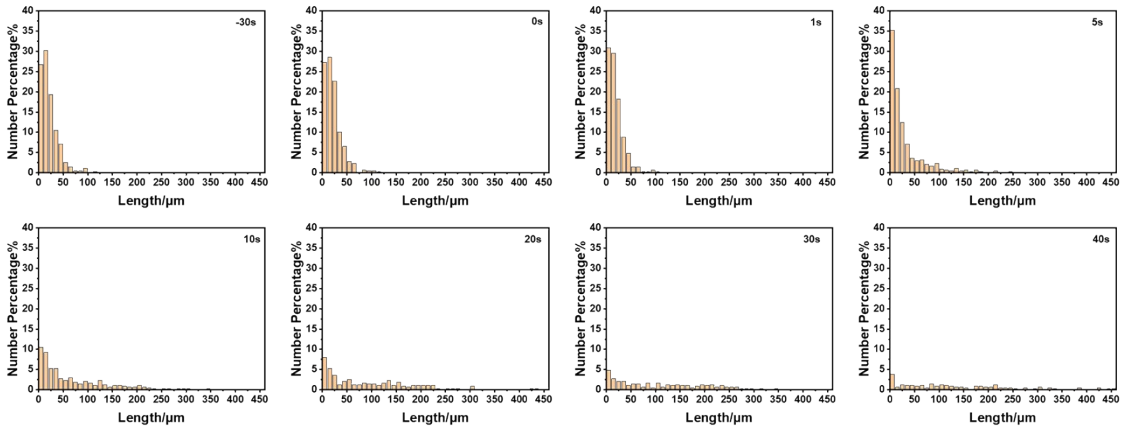

Figure S5. Variation in particle chain length of S-Fe_3O_4@Au/PDA.

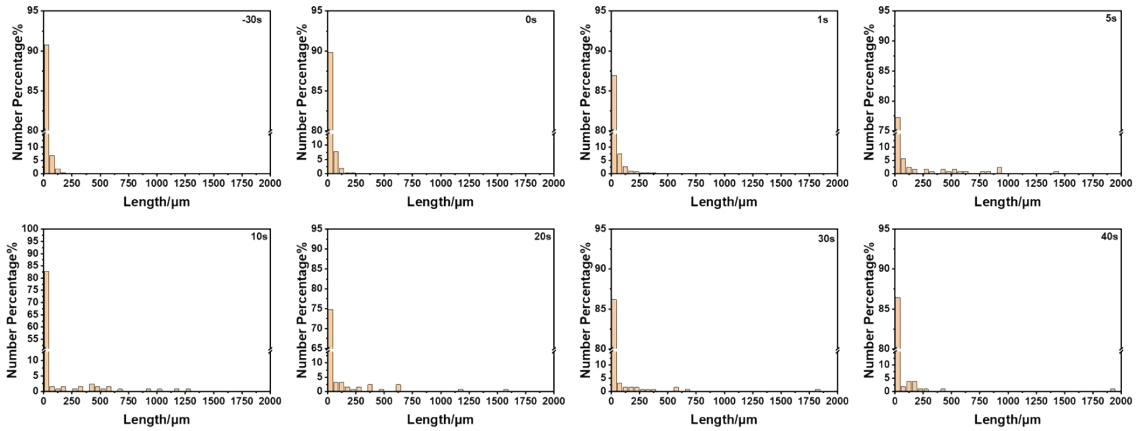

Figure S6. Variation in particle chain length of L-Fe_3O_4@Au/PDA.

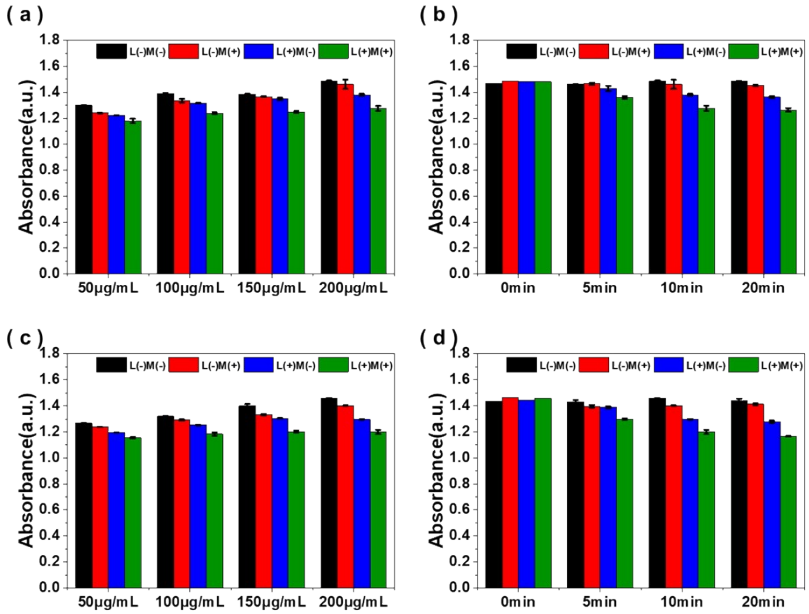

Figure S7. OD600 values of *S. aureus* treated with S-Fe_3O_4@Au/PDA (a-b) and L-Fe_3O_4@Au/PDA (c-d) at different concentrations and durations.

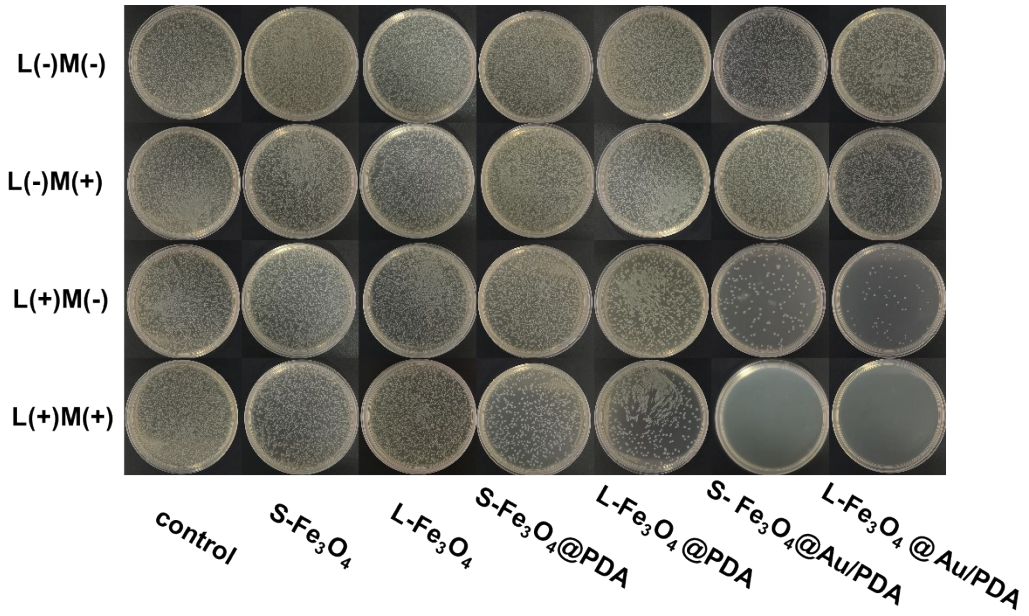

Figure S8. Photographs of *E. coli* colonies treated with Fe_3O_4, Fe_3O_4@PDA and Fe_3O_4@Au/PDA (200 μg/mL) for 10 min under various conditions.

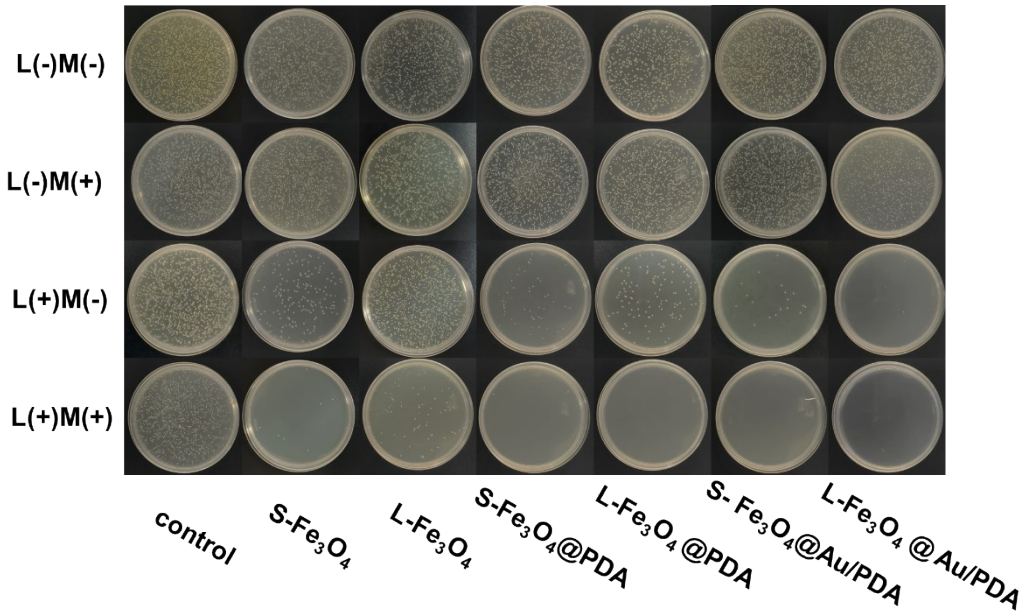

Figure S9. Photographs of *S. aureus* colonies treated with Fe_3O_4, Fe_3O_4@PDA and Fe_3O_4@Au/PDA (200 μg/mL) for 10 min under various conditions.